hydrology

MDPI

Article

Flood Risk Analysis in Lower Part of Markham River Based on Multi-Criteria Decision Approach (MCDA)

Sailesh Samanta [1,*], Cathy Koloa [2], Dilip Kumar Pal [2] and Babita Palsamanta [3]

1 GIS Section, Department of Surveying and Land Studies, The PNG University of Technology, Private Mail Bag, Lae 411, Morobe Province, Papua New Guinea
2 Department of Surveying and Land Studies, The PNG University of Technology, Private Mail Bag, Lae 411, Morobe Province, Papua New Guinea; cmkoloa@gmail.com (C.K.); dkpal200090@gmail.com (D.K.P.)
3 The PNG University of Technology Campus, Private Mail Bag, Lae 411, Morobe Province, Papua New Guinea; mundey2@gmail.com
* Correspondence: rsgis.sailesh@gmail.com or ssamanta@survey.unitech.ac.pg; Tel.: +675-473-4977; Fax: +675-475-7667

Academic Editor: Luca Brocca
Received: 24 June 2016; Accepted: 27 July 2016; Published: 2 August 2016

Abstract: Papua New Guinea is blessed with a plethora of enviable natural resources, but at the same time it is also cursed by quite a few natural disasters like volcanic eruptions, earthquakes, landslide, floods, droughts etc. Floods happen to be a natural process of maintaining the health of the rivers and depth of its thalweg; it saves the river from becoming morbid while toning up the fertility of the riverine landscape. At the same time, from human perspective, all these ecological goodies are nullified when flood is construed overwhelmingly as one of the most devastating events in respect to social and economic consequences. The present investigation was tailored to assess the use of multi-criteria decision approach (MCDA) in inland flood risk analysis. Categorization of possible flood risk zones was accomplished using geospatial data sets, like elevation, slope, distance to river, and land use/land cover, which were derived from digital elevation model (DEM) and satellite image, respectively. A pilot study area was selected in the lower part of Markham River in Morobe Province, Papua New Guinea. The study area is bounded by 146°31′ to 146°58′ east and 6°33′ to 6°46′ south; covers an area of 758.30 km^2. The validation of a flood hazard risk map was carried out using past flood records in the study area. This result suggests that MCDA within GIS techniques is very useful in accurate and reliable flood risk analysis and mapping. This approach is convenient for the assessment of flood in any region, specifically in no-data regions, and can be useful for researchers and planners in flood mitigation strategies.

Keywords: GIS; rating; weight; multi-criteria decision approach; flood risk mapping

1. Introduction

Heavy rain, especially over the upper catchment, in a short period of time causes flooding or flash flooding in the lower catchment. Flooding is a natural disaster caused by high intensity downpours. A flood occurs when overland flow of waters inundate land and may cause damage to crops, damage to infrastructure, or even loss of human lives [1,2]. More than 140 million people are affected each year in the world due to flood [3]. Flood management and mitigation are vital to the physical and social environment of a nation, which assumes an important role in economic development [4,5]. Flooding can be classified into three different categories based on how fast it is occurring like (i) flash floods, which occur due to heavy rain for a few hours and with little or no warning and disperse quickly, (ii) rapid onset floods, that happen with several hours of heavy rainfall and can last for several days, and (iii) slow onset floods, which occur gradually over a fairly long

period of time [6]. Flood risk mapping and hazard analysis for any watershed or drainage basin engage several factors or parameters and criteria [7,8]. Geographic information system (GIS) and remote sensing (RS) techniques have made significant contributions in natural hazard analysis [9,10]. During the last few decades, researchers were involved in developing different methods and models for natural hazard mapping using RS and GIS techniques [11,12]. Frequency ratio [13,14], analytical hierarchy process [15], fuzzy logic [16], logistic regression [17], artificial neural networks [18–20] and weights-of-evidence [21], and multi-criteria decision support systems [22,23] are a few well known and acceptable methods in natural hazard modelling for analyzing complex problems in different regions. MCDA and GIS have been familiarized as an imperative tool in spatial data analysis and mapping [24,25]. This research is focussed on assessing the use of an MCDA approach in inland flood risk analysis based on four different geospatial data sets, like elevation, slope, distance to river, and land use/land cover. This research was conducted in the lower part of the Markham River in Morobe Province, Papua New Guinea.

2. Study Area and Materials Used

The study area includes a geographical area extending from 146°31′ to 146°58′ east and 6°33′ to 6°46′ south and envelops an area of 758.30 km^2. The area is located in the lower part of Markham River in the Morobe Province of Papua New Guinea (Figure 1). The upper catchment area of Markham is dominated by primary forests and rugged mountains with steep slopes [26]. Markham river is the fourth longest river in Papua New Guinea originated from Finisterre range (457 m) and gets emptied into Huon Gulf after 180 km of checkered path. Erap River from the Saruwage range (from the northern side) and Watut from Wau-Bulolo (from the southern side) are two major tributary rivers of the Markham (Figure 1). The upper catchment area of the Markham is dominated by primary forests and rugged mountains with steep slopes. Absence of any soil conservation measure exacerbated by commercial logging, mining, and small scale mining on the river for alluvial gold extraction are the major economic activities which cause accelerated soil erosion within the catchment area. The study area is characterized with tropical humid climate with an average rainfall of 4200 mm. The Markham carries flows from the 12,450 km^2 catchment with huge mobile bed load ranging from fine silt to cobbles [27]. The lower catchment of the Markham River has a wider valley ranging in width between 3 km and 8 km. In last two decades, the area has been subjected to several destructive floods, which were chosen as verification sites for finalizing flood risk zoning. Final 58 km flow of the Markham River starts from the Watut junction to the mouth (Huon gulf) and the average 7.5 km distance from the river on each side was considered for hosting this research (Figure 1- bottom: sketch on satellite data).

Identification of possible flood risk zones was performed using geospatial data sets, like elevation, slope, distance to river, and land use/land cover. These parameters were derived from digital elevation model (DEM) and satellite image respectively. Optical bands with false color combination of Landsat 8, operational land imager (OLI) was used to derived land use/land cover of the study area. River lines were digitized from the satellite image and used to find the distance from river. One of the most widely used high-resolution topographic data or Digital Elevation Model (DEM) source is advanced space borne thermal emission and reflection radiometer (ASTER) mission. ASTER provides topographic data in 30-meter spatial resolution. All other details of the data sets are given in the Table 1.

Table 1. Data sets used for Identification of possible flood risk zones.

Sl No	Data Type	Resolution	Year	Source
1	LANDSAT-8, OLI	15 m Pan-Sharpen	2013	Department of Surveying and Land Studies,
2	ASTER-DEM	30 m	2001	The PNG University of Technology
3	Village locations and population data sets of Morobe	Point and statistics	2009	Geobook, PNGRIS
4	Historical flood magnitude	Point location	2002 to 2006	GFDS, Version 2 http://www.gdacs.org/

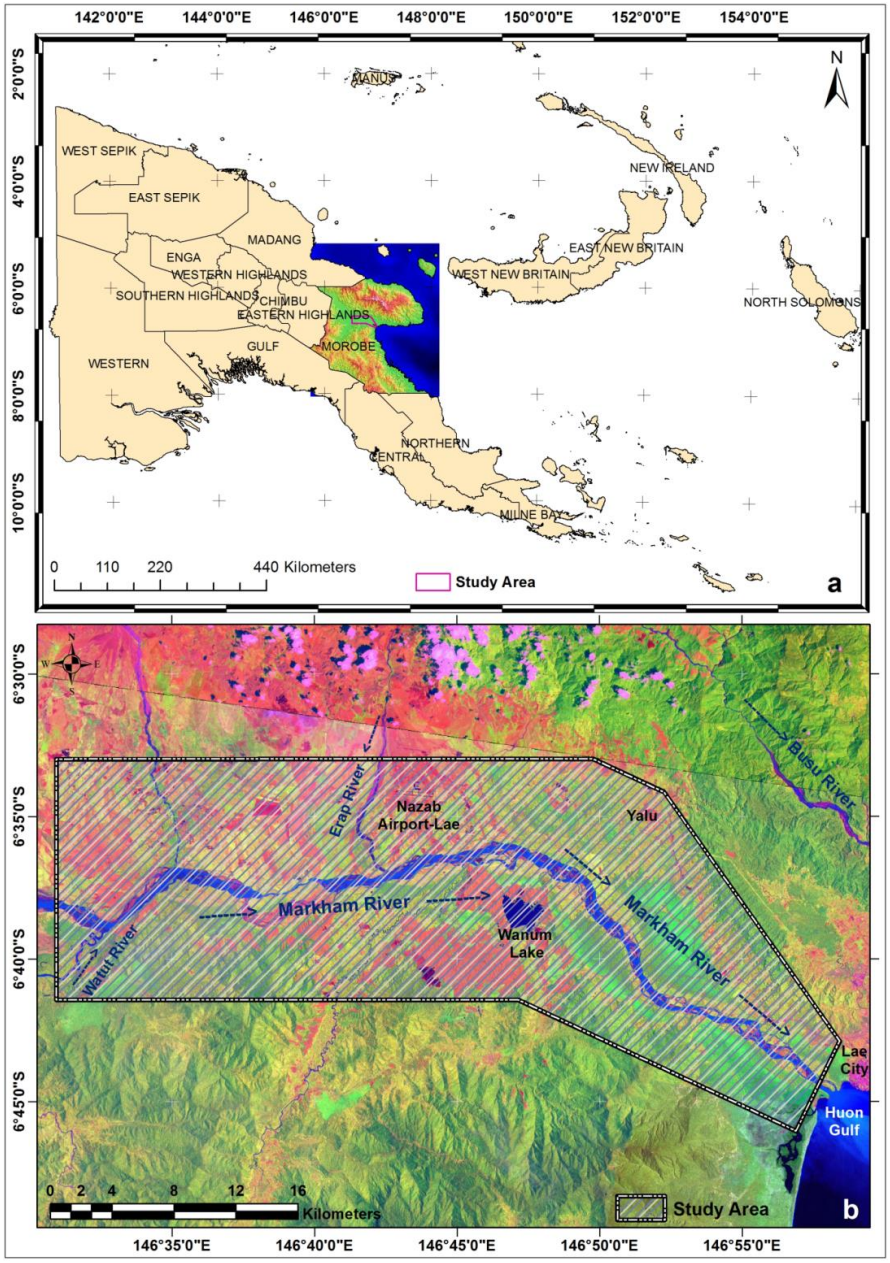

Figure 1. Location map of the study area.

3. Methodology

To generate a flood risk map in the lower catchment of a drainage basin, the area selection of effective parameters is vital [19,28]. Although it is difficult to choose factors unanimously to be applied in flood susceptibility assessments, some important variables have a definitive role in flood risk mapping as mentioned by many researchers [29]. Different geospatial data sets, such as elevation, slope, distance to river, and land use/land cover were considered as dependent parameters. Landsat 8, OLI (Path/Row of 96/65 with a spatial resolution of 15 m Pan-sharpen) satellite image was used to digitize river lines in the study area (Figure 2a).

Elevation plays a vital role on the spread of flooding and depth [30] of flood in the lower catchment area. Slope is another independent parameter which can accelerate the soil erosion and surface runoff as well as vertical percolation [31]. Both parameters, elevation and degree slope were derived from ASTER DEM (30 m spatial resolution) in ArcGIS 3-D analysis extension (Figure 2b,c).

Elevation database was reclassified into nine groups within a given range, namely less than 20, 20–40, 40–60, 60–80, 80–100, 100–200, 200–300, 300–500, and more than 500 m (Figure 2b). The slope in degree database was categorized into nine groups, such as less than 1, 1–2, 2–3, 3–4, 4–5, 5–10, 10–15, 15–20, and more than 20° (Figure 2c).

Floodplains and the areas in the vicinity of river are the most affected areas during floods [32]. Proximity analysis in ArcGIS was used to produce distance from river data sets. Nine different distance class were generated (Figure 2d) with a specific interval of distance, such as - up to 100, 100–200, 200–300, 300–400, 400–500, 500–750, 750–1000, 1000–2000, and more than 2000 m.

Infiltration or the vertical downward movement of water has profound bearing on the incidence of floods. Areas dominated by vegetation, especially tree vegetation/forests, which are known for inducing high infiltration rates, have eventually low susceptibility to flooding, thus have a negative relationship of flood occurrence and vegetation density. Surface runoff is very high in urban and built-up areas because of impervious surfaces. So land use/land cover is an important factor for flood susceptibility mapping [33]. Land use/land cover characteristics of the study area were analyzed following maximum likelihood algorithm of supervised classification in Erdas Imagine software v11 [34]. The entire study area was classified into 10 classes, such as inland water, river water, river course shrub, river course grass, river course vegetation, other shrub, other grass, low density vegetation, dense vegetation, and impervious road cum built-up areas (Table 2 and Figure 2e).

Table 2. Land use/land cover characteristics generated from satellite image using supervised classification.

Value	Land Use/Land Cover Classes	Area (km^2)	% Area
1	Inland Water	3.55	0.47
2	River Water	35.82	4.72
3	River Course Shrub	25.10	3.31
4	River Course Grass	20.81	2.74
5	River Course Vegetation	33.73	4.45
6	Other Shrub	91.49	12.07
7	Other Grass	152.86	20.16
8	Low Dense Vegetation	48.33	6.37
9	Dense Vegetation	340.75	44.94
10	Road and Built-up	5.86	0.77

Different rates for all the classes under each parameters and weights for the parameters were assigned simultaneously to take a final decision on suitable rates and weights, which produced better results. The pair wise comparisons of all the parameters were taken as the inputs while the relative weights and rates of the parameters and sub classes were the outputs. After preparation of all parameters and their individual class, user defined rate (R) [35] on a scale of 1 to 9 [36] were assigned depending on their significance or influence on flood risk. The highest rate of 9 refers to extreme vulnerability to flood risk and rate of 1 refers to almost no risk. For example, the probability of flood occurrences and intensity are high close to the river [32], so the rank of 9 was assigned to the areas which are located within 100 m distance from the main river. Normalized rating index (NRI) was calculated using total rate dividing with individual rate. Based on the individual significance a total weight (W) of 10 was assigned after divided amongst all four parameters. Weight of 4 was assigned to the distance from river because the most affected areas during floods are those near the river, as a consequence of bank overflow [32]. Slope of the land plays an important role in determining surface runoff velocity and rate of vertical percolation and a W value of 3 was assigned to this parameter. Altitude has an important impact on the spread of flooding and has a key role in the control of the direction of overflow movement and also in the depth of the flood. A W value of 2 was assigned to this parameters. Normalized weight index (NWI) was calculated using total weight dividing with individual weight as shown in Table 3. Figure 3 shows the detailed methodology adopted in this research.

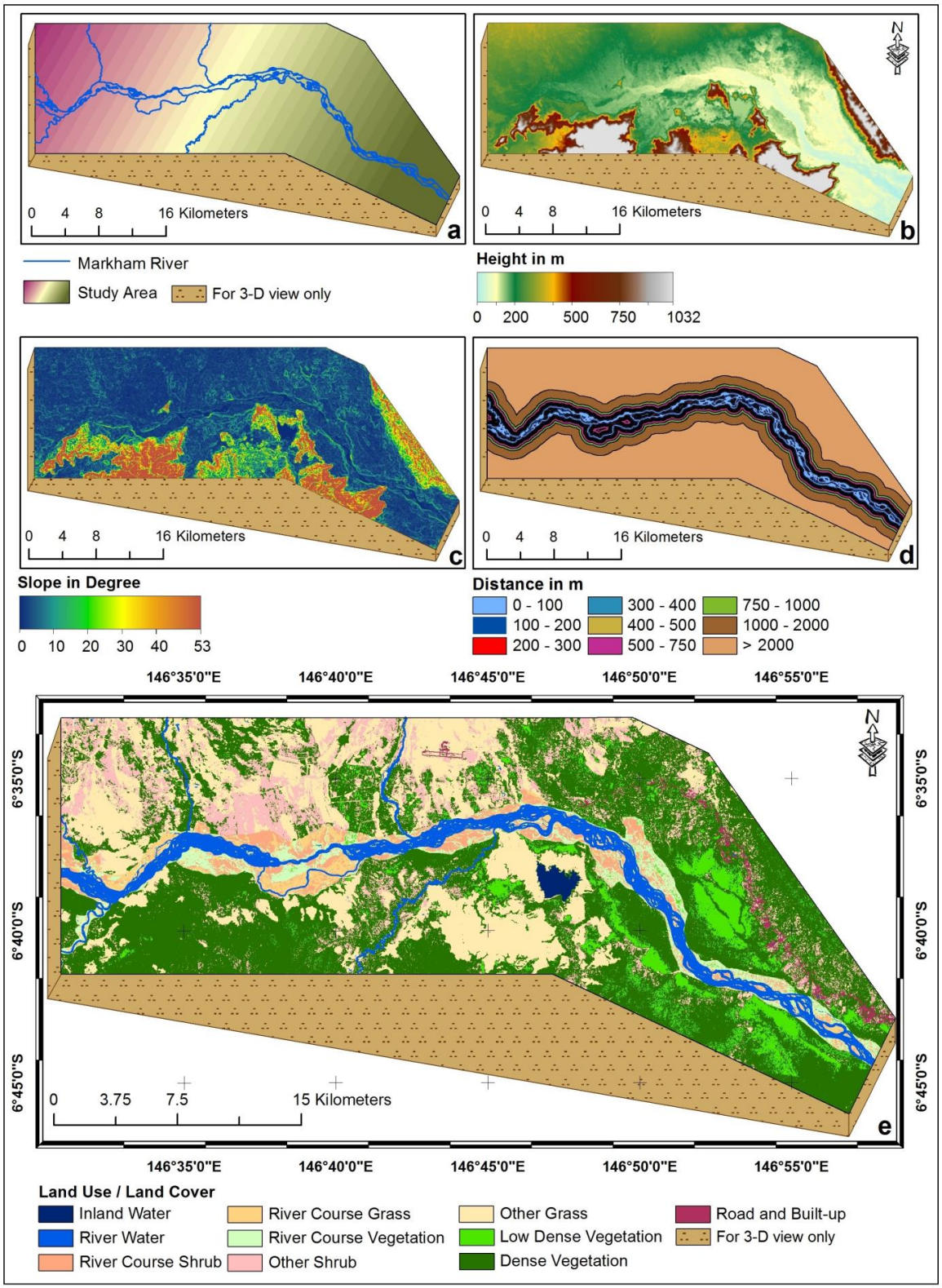

Figure 2. Markham river (**a**); digital elevation model (**b**); slope in degree (**c**); distance from river (**d**); and land use/land cover characteristics (**e**), derived from ASTER-DEM and Landsat 8, OLI satellite image.

Table 3. Rate, normalized rating index, weight index based on MCDA.

Parameters	Category/Class	Rate (R)	Normalized Rating Index (NRI) [Individual/Total]	Weight (W)	Normalized Weight Index (NWI)
Elevation (in m)	<20	9	0.20	2	0.2
	20–40	8	0.18		
	40–60	7	0.16		
	60–80	6	0.13		
	80–100	5	0.11		
	100–200	4	0.09		
	200–300	3	0.07		
	300–500	2	0.04		
	More than 500	1	0.02		
	Total	45	1.00		
Slope (in Degree)	<1	9	0.20	3	0.3
	1 to 2	8	0.18		
	2 to 3	7	0.16		
	3 to 4	6	0.13		
	4 to 5	5	0.11		
	5 to 10	4	0.09		
	10 to 15	3	0.07		
	15 to 20	2	0.04		
	More than 20	1	0.02		
	Total	45	1.00		
Distance from River (in m)	<100	9	0.20	4	0.4
	100–200	8	0.18		
	200–300	7	0.16		
	300–400	6	0.13		
	400–500	5	0.11		
	500–750	4	0.09		
	750–1000	3	0.07		
	1000–2000	2	0.04		
	More than 2000	1	0.02		
	Total	45	1.00		
Land Use/Land Cover	Inland Water	N/A	N/A	1	0.1
	River Water	9	0.20		
	River Course Shrub	8	0.18		
	River Course Grass	7	0.16		
	River Course Vegetation	6	0.13		
	Road and Built-up	5	0.11		
	Other Shrub	4	0.09		
	Other Grass	3	0.07		
	Low Dense Vegetation	2	0.04		
	Dense Vegetation	1	0.02		
	Total	45	1.00		

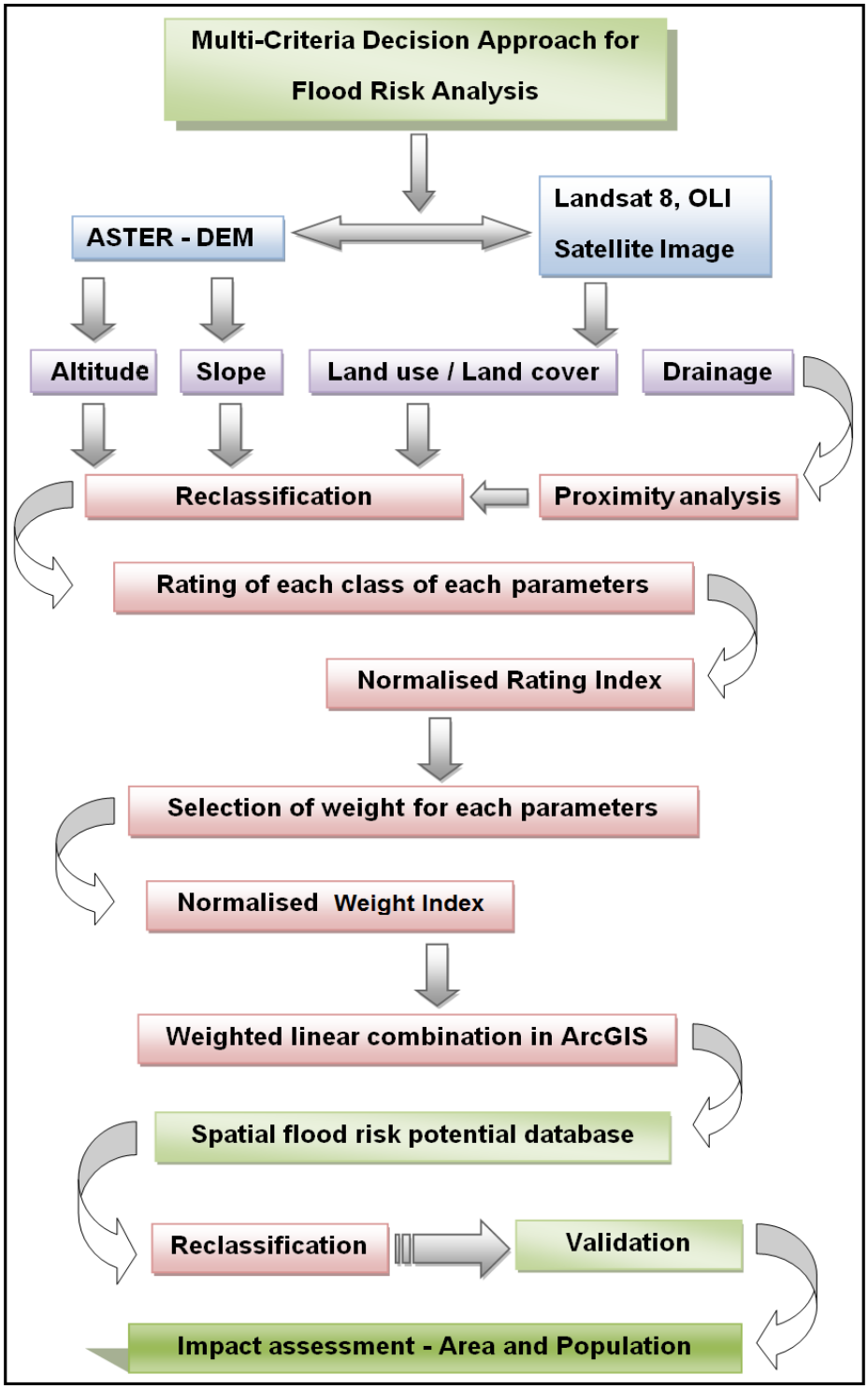

Figure 3. Methodological flow chart for flood risk analysis through MCDA.

4. Result and Discussions

4.1. Land Use/Land Cover

The land use/land cover map shows that the area is mostly dominated by dense vegetation, which covered an area of 340.75 km^2 and it is about 45% of the total area (Table 2 and Figure 2e). Lae city is located outside of the study area as it is sitting within another drainage basin, but the extension of the

city (roads and other nearby developments) towards Nazab airport is within the study area, covering an area of 5.86 km^2 (0.77%) (Table 2 and Figure 2e). Other land use/land covers classes, like inland water covered an area of 3.55 km^2 (0.47%), river water 35.82 km^2 (4.72%), river course shrub 25.10 km^2 (3.31%), river course grass 20.81 km^2 (7.74%), other shrub 91.49 km^2 (12.07%), other grass 152.86 km^2 (20.16%), and low density vegetation 48.33 km^2 (6.37%). The overall classification accuracy and kappa statistics were derived as 91.5 % and 0.85, respectively.

4.2. Elevation and Slope

Maximum altitude of 1032 m and slope of 53° are found in the southern part of study area indicating rugged terrain, whereas going towards the east it became very gentle/smooth (Figure 2b,c). Both elevation database and slope data sets were reclassed into nine groups. Elevation classes 100 to 200, 200 to 300, and 300 to 400 m cover total area of 466.05 km^2 (61.46%). About 40.63 km^2 (5.36%) area are located above 500 m from mean sea level where flood risk is about zero. Other classes that ranged up to 100 m altitude covered an approximate area of 251.62 km^2 (44.31%) and are marked as high potential to flood. Slope classes above 10° occupy total area of 490.52 km^2 (64.69%), which are marked as 'no risk' zones. About 218.77 km^2 (28.85%) area consist in low slope terrain, which ranged up 5° are considered as 'high risk' zone of flood. All statistics related to different classes of elevation and slope are summarized in Table 4.

Table 4. Elevation and slope characteristics of the study area after reclassification.

Elevation (m)	Area (km^2)	Percentage	Slope (degree)	Area (km^2)	Percentage
<20	16.67	2.20	< 1	53.26	7.02
20–40	26.08	3.44	1 to 2	34.87	4.60
40–60	38.89	5.13	2 to 3	40.5	5.34
60–80	78.58	10.36	3 to 4	62.58	8.25
80–100	91.4	12.05	4 to 5	27.56	3.63
100–200	170.65	22.50	5 to 10	49.01	6.46
200–300	171.52	22.62	10 to 15	100.45	13.25
300–500	123.88	16.34	15 to 20	203.94	26.89
More than 500	40.63	5.36	More than 20	186.13	24.55
Total	758.3	100.00	Total	758.3	100.00

Weighted sum operation in spatial analysis extension of ArcGIS 10 was followed to integrate all NRI and NWI (Table 3) and to generate a pixel by pixel (30 m spatial resolution) flood risk/susceptibility database (Figure 4a). Flood risk index values of the output database range from 0.22 (Low) to 2.00 (high). Flood risk data was reclassified into five categories through a manual classification method as: (i) no risk (0.22–0.50), low risk (0.50–1.00), medium risk (1.00–1.50), high risk (1.50–1.75), and very high risk (1.75–2.00) (Table 5 and Figure 4b). 'No risk' refers to zones where the chances of flood occurrences are about zero and 'high' and 'very high' risk refer to the plausible areas where flood can eventuate due to seasonal as well as sporadic heavy rainfall (might be El Nino/Southern Oscillation induced episodes that have the potential to capture both 'high' and 'medium' risk areas). The 'medium' risk is considered along the areas that might be seasonally inundated in the wet season [37,38].

Finally spatial analysis tools of ArcGIS v-10 are used to calculate inundated area, villages, total population, and road infrastructure that are coming under different flood risk zone. The flood risk map shows that about 88.44 km^2 (11.66%) of area on both sides of the Markham River is highly vulnerable as it falls under high to very high risk zones (Table 5 and Figure 4). About 249.17km^2 (32.86%) of area is moderately vulnerable and falls under medium risk. According to population statistics and road infrastructure of year 2008 [37,38], 8.50 km of road and four villages (population size of 1490) are marked as highly vulnerable as they come under 'high' and 'very high' flood risk zones (Table 5 and Figure 5). On the other hand, 58.88 km of road and 35 villages (population size of 16,584) are moderately vulnerable, which are situated under medium flood risk zones (Table 5 and Figure 5).

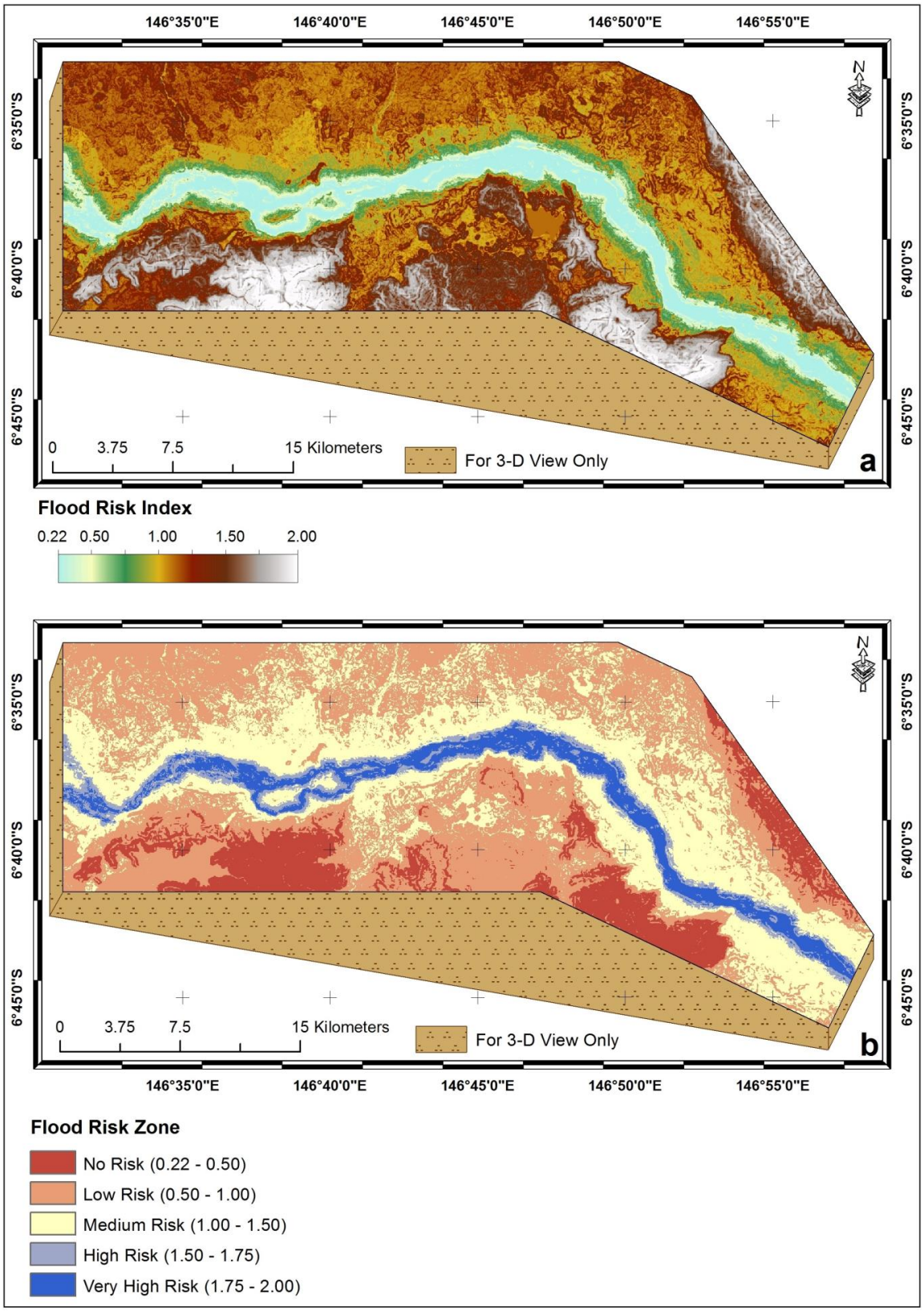

Figure 4. Flood risk analysis map based MCDA- resulted flood risk index (**a**) and classified flood risk zones (**b**).

Table 5. Flood risk index and its impact based on MCDA for FRA mapping.

Value	Flood Risk	Flood Risk Index Value	Area (km^2)	Area (%)	No of Village	Population	Length of Road (km)
1	No Risk	0.22–0.50	90.97	12.00	NA	NA	2.28
2	Low Risk	0.50–1.00	329.72	43.48	60	23282	89.66
3	Medium Risk	1.00–1.50	249.17	32.86	35	16584	58.88
4	High Risk	1.50–1.75	40.98	5.40	3	1328	6.55
5	Very High Risk	1.75–2.00	47.46	6.26	1	162	1.95

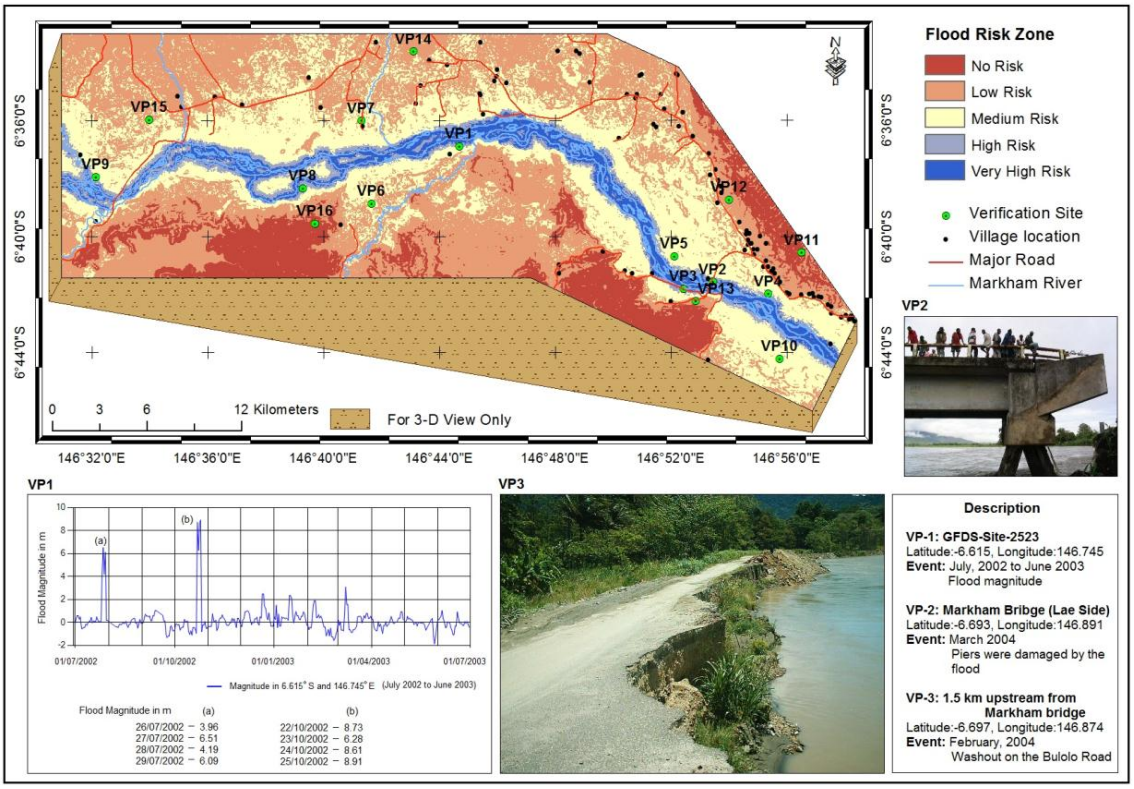

Figure 5. Validation of flood risk analysis at different sites with historical flood events and its vulnerability.

Historical floods events were used as verification sites (VP1 to VP3) to validate the output generated through flood risk analysis. VP1 to VP3 are stationed on the high to very high flood risk zone (Figure 5) based on flood risk analysis through MCDA. Figure 5 shows three different extremes flood events and the damages within the study area. Extreme flood magnitudes were measured during 2012 at GFDS, site 2523 (VP1 - location: 6.615° S, 146.745° E) by global flood detection system [39]. The second verification point is located about at the end of the Markham Bridge (VP2 - 6.693° S, 146.891° E) and had experienced a devastating flood in March 2004. A portion of the bridge, the abutment and the piers were damaged on the approach road to the Lae city (Figure 5). Another flood incident occurred in the same year (February-2004) at 1.5 km upstream from Markham Bridge (VP3 - 6.697° S, 146.874° E). 120 m road was washed out (on Lae-Bulolo road) in this event (Figure 5). The peak discharge was estimated as in the range 2600 m^3/s to 3200 m^3/s and peak flood velocity as 3.4 m/s respectively in the main channel near Markham Bridge during this event [27]. Another set of validation points (VP4 to VP16) were collected from inundation characteristics layer of PNGRIS database of Papua New Guinea [38] to validate of flood hazard risk map. Validation points, VP4 to VP10 are characterized by periodic flooding. Periodic flooding refers to the areas which are

generally flooded for 3 to 4 days or less as a result of brief spate river or short term breach of river bank due to intensive rainfall events. According to flood risk map VP4 to VP10 are marked as 'high' to 'moderate' flood risk. Finally six other validation points (VP11 to VP16) are characterized as no flooding or inundation based on the PNGRIS database [38] which are situated in areas of either 'low risk' or 'no risk' of flooding based on the analysis output through MCDA (Table 6).

Table 6. Validation of flood risk map through MCDA.

Validation Point (VP)	Ground Observation/Existing Data Base	Flood Risk Analysis
VP1	Flood, 2012	High
VP2	Flood, 2004	Very high
VP3	Flood, 2004	Very high
VP4	Periodic flooding [38]	High
VP5		Moderate
VP6		Moderate
VP7		Moderate
VP8		High
VP9		High
VP10		Moderate
VP11	No flooding or inundation [38]	No risk
VP12		Low risk
VP13		Low risk
VP14		Low risk
VP15		Low risk
VP16		No risk

5. Conclusion

In this research, a flood risk map was developed based on multi-criteria decision approach (MCDA) using different geospatial data sets, like elevation, slope, distance to river, and land use/land cover. The validation report suggests that MCDA and GIS techniques are very powerful methods in flood risk analysis and mapping. The MCDA approach used in this study can be enhanced further after including many more parameters like rainfall, surface runoff, river discharge, river channel morphology, etc. The same can be used for flood preparedness and mitigation activities in any region, like in a river basin as a hydrological unit or particularly in no-data regions. As the most damaged were found close to the Markham bridge which connect Lae city and Bulolo town. It can be mentioned that a part of the Lae city also appears a bit vulnerable where it is quite close to the Markham River. The river bank protection strategy can be adopted by constructing suitable dykes. Diversion of channels can also be another option through the mid-stream island near to the bridge on the Markham river.

Acknowledgments: Authors are thankful to the PNGUNITECH (Papua New Guinea University of Technology) and to the Department of Surveying and Land Studies for all the facilities made available and availed for the research work. Satellite digital data available from USGS Global Land Cover Facility and used in this study is also duly acknowledged. The authors gratefully acknowledge the anonymous reviewers for providing their critical comments to improve the quality of this manuscript.

Author Contributions: All authors contributed to the conception of the study; S.S., B.P. designed the methodology and wrote the manuscript; C.K. assembled the input data; and D.K.P shared expert knowledge of the study area and made necessary corrections to the manuscript.

Conflicts of Interest: The authors declare no conflict of interest.

References

1. Merz, B.; Kreibich, H.; Schwarze, R.; Thieken, A. Assessment of economic flood damage. *Nat. Hazard Earth Syst. Sci.* **2010**, *10*, 1697–1724. [CrossRef]

2. Hudson, P.; Botzen, W.J.W.; Kreibich, H.; Bubeck, P.; Aerts, J.C.J.H. Evaluating the effectiveness of flood damage mitigation measures by the application of propensity score matching. *Nat. Hazards Earth Syst. Sci.* **2014**, *14*, 1731–1747. [CrossRef]
3. WHO-World Health Organization. *Disaster Data-key Trends and Statistics in World Disasters Report*; WHO: Geneva, Switzerland, 2003. Available online: http://www.ifrc.org/PageFiles/89755/2003/43800-WDR2003_En.pdf (accessed on 5 April 2016).
4. Huang, X.; Tan, H.; Zhou, J.; Yang, T.; Benjamin, A.; Wen, S.W.; Li, S.; Liu, A.; Li, X.; Fen, S.; Li, X. Flood hazard in Hunan province of China: An economic loss analysis. *Nat. Hazards* **2008**, *47*, 65–73. [CrossRef]
5. Markantonis, V.; Meyer, V.; Lienhoop, N. Evaluation of the environmental impacts of extreme floods in the Evros River basin using Contingent Valuation Method. *Nat. Hazards* **2013**, *69*, 1535–1549. [CrossRef]
6. Samanta, S.; Koloa, C. Modelling Coastal Flood Hazard Using ArcGIS Spatial Analysis tools and Satellite Image. *Int. J. Sci. Res.* **2014**, *3*, 961–967.
7. Xu, C.; Chen, Y.; Chen, Y.; Zhao, R.; Ding, H. Responses of surface runoff to climate change and human activities in the arid region of Central Asia: A case study in the Tarim River Basin, China. *Environ. Manag.* **2013**, *51*, 926–938. [CrossRef] [PubMed]
8. Poussin, J.K.; Botzen, W.J.W.; Aerts, J.C.J.H. Factors of influence on flood damage mitigation behavior by households. *Environ. Sci. Policy* **2014**, *40*, 69–77. [CrossRef]
9. Patel, D.P.; Srivastava, P.K. Flood hazards mitigation analysis using remote sensing and GIS: Correspondence with town planning scheme. *Water Resour. Manag.* **2013**, *27*, 2353–2368. [CrossRef]
10. Moel, H.D.; Vliet, M.V.; Aerts, J.C.J.H. Evaluating the effect of flood damage-reducing measures: A case study of the unembanked area of Rotterdam, the Netherlands. *Reg. Environ. Change* **2014**, *14*, 895–908.
11. Althuwaynee, O.F.; Pradhan, B.; Park, H.J.; Lee, J.H. A novel ensemble bivariate statistical evidential belief function with knowledge-based analytical hierarchy process and multivariate statistical logistic regression for landslide susceptibility mapping. *Catena* **2014**, *114*, 21–36. [CrossRef]
12. Van, W.C.J.; Rengers, N.; Soeters, R. Use of geomorphological information in indirect landslide susceptibility assessment. *Nat. Hazards* **2003**, *30*, 399–419.
13. Lee, M.J.; Kang, J.E.; Jeon, S. Application of frequency ratio model and validation for predictive flooded area susceptibility mapping using GIS. In Proceedings of the Geoscience and Remote Sensing Symposium (IGARSS), Munich, Germany, 22–27 July 2012; pp. 895–898.
14. Tehrany, M.S.; Pradhan, B.; Mansor, S.; Ahmad, N. Flood susceptibility assessment using GIS-based support vector machine model with different kernel types. *Catena* **2015**, *125*, 91–101. [CrossRef]
15. Stefanidis, S.; Stathis, D. Assessment of flood hazard based on natural and anthropogenic factors using analytic hierarchy process (AHP). *Nat. Hazards* **2013**, *68*, 569–585. [CrossRef]
16. Pradhan, B. Use of GIS-based fuzzy logic relations and its cross application to produce landslide susceptibility maps in three test areas in Malaysia. *Environ. Earth Sci.* **2011**, *63*, 329–349. [CrossRef]
17. Pradhan, B. Flood susceptible mapping and risk area delineation using logistic regression, GIS and remote sensing. *J. Spat. Hydrol.* **2010**, *9*, 1–18.
18. Samanta, S.; Pal, D.K.; Lohar, D.; Pal, B. Interpolation of climate variables and temperature modeling. *Theor. Appl. Climatol.* **2012**, *107*, 35–45. [CrossRef]
19. Kia, M.B.; Pirasteh, S.; Pradhan, B.; Rodzi, M.A.; Sulaiman, W.N.A.; Moradi, A. An artificial neural network model for flood simulation using GIS: Johor River Basin, Malaysia. *Environ. Earth Sci.* **2012**, *67*, 251–264. [CrossRef]
20. Lohani, A.K.; Goel, N.K.; Bhatia, K.K.S. Improving real time flood forecasting using fuzzy inference system. *J. Hydrol.* **2014**, *509*, 25–41. [CrossRef]
21. Tehrany, M.S.; Pradhan, B.; Jebur, M.N. Flood susceptibility mapping using a novel ensemble weights-of-evidence and support vector machine models in GIS. *J. Hydrol.* **2014**, *512*, 332–343. [CrossRef]
22. Koloa, C.; Samanta, S. Development Impact Assessment Along Merkham River through Remote Sensing and GIS Technology. *Int. J. Asian Acad. Res. Ass.* **2013**, *5*, 26–41.
23. Malczewski, J. GIS-based multicriteria decision analysis: A survey of the literature. *Int. J. Geogr. Inf. Sci.* **2006**, *20*, 703–726. [CrossRef]
24. Scheuer, S.; Haase, D.; Meyer, V. Exploring multicriteria flood vulnerability by integrating economic, social and ecological dimensions of flood risk and coping capacity: From a starting point view towards an end point view of vulnerability. *Nat. Hazards* **2011**, *58*, 731–751. [CrossRef]

25. Solin, L. Spatial variability in the flood vulnerability of urban areas in the headwater basins of Slovakia. *Flood Risk Manag.* **2012**, *5*, 303–320. [CrossRef]
26. Pal, B.; Samanta, S.; Pal, D.K. Morphometric and Hydrological analysis and mapping for Watut watershed using Remote Sensing and GIS techniques. *Int. J. Adv. Eng. Technol.* **2012**, *2*, 357–368.
27. Tilley, J.R.; Kell, R.A.M.; Haro, A. Protecting the Markham Bridge, Morobe Province, PNG. In Proceedings of the 9th International River Symposium, Brisbane, Australia, 4–7 September 2006.
28. Manandhar, B. Flood Plain Analysis and Risk Assessment of Lothar Khola. M.Sc. Thesis, Tribhuvan University, Phokara, Nepal, 2010. p. 64.
29. Tehrany, M.S.; Lee, M.J.; Pradhan, B.; Jebur, M.N.; Lee, S. Flood susceptibility mapping using integrated bivariate and multivariate statistical models. *Environ. Earth Sci.* **2014**, *72*, 4001–4015. [CrossRef]
30. Stieglitz, M.; Rind, D.; Famiglietti, J.; Rosenzweig, C. An efficient approach to modeling the topographic control of surface hydrology for regional and global climate modeling. *J. Clim.* **1997**, *10*, 118–137. [CrossRef]
31. Youssef, A.M.; Pradhan, B.; Hassan, A.M. Flash flood risk estimation along the St. Katherine road, southern Sinai, Egypt using GIS based morphometry and satellite imagery. *Environ. Earth Sci.* **2011**, *62*, 611–623. [CrossRef]
32. Fernandez, D.S.; Lutz, M.A. Urban flood hazard zoning in Tucumán Province, Argentina, using GIS and multicriteria decision analysis. *Eng. Geol.* **2010**, *111*, 90–98. [CrossRef]
33. Norman, L.M.; Huth, H.; Levick, L.; Burns, I.S.; Phillip, G.D.; Lara-Valencia, F.; Semmens, D. Flood hazard awareness and hydrologic modelling at Ambos Nogales, United states-Mexico border. *Flood Risk Manag.* **2010**, *3*, 151–165. [CrossRef]
34. Samanta, S.; Pal, D.K. Change Detection of Land Use and Land Cover over a Period of 20 Years in Papua New Guinea. *Nat. Sci.* **2016**, *8*, 138–151. [CrossRef]
35. Elizabeth, A.; Samanta, S. Landslide vulnerability mapping (LVM) using weighted linear combination (WLC) model through remote sensing and GIS techniques. *J. Model. Earth Syst. Environ.* **2016**, *2*, 1–14.
36. Saaty, T.L. *The Analytic Hierarchy Process: Planning, Priority Setting, Resource Allocation*; McGraw-Hill: New York, NY, USA, 1980.
37. Geobook. *Provincial GIS-based Planning Tools*; The Remote Sensing Centre of University of Papua New Guinea: Port Moresby, Papua New Guinea, 2009.
38. PNGRIS-Papua New Guinea Resource Information System. *The Land-Use Section, Science and Technology Branch, Department of Agriculture and Livestock*, 3rd ed.; University of Papua New Guinea: Boroko, Papua New Guinea, 2009.
39. Kugler, Z.; Groeve, T.D. *The Global Flood Detection system*; EUR 23303 EN; Office for Official Publications of the European Communities: Ispra, Italy, 2007; pp. 1–45.

© 2016 by the authors; licensee MDPI, Basel, Switzerland. This article is an open access article distributed under the terms and conditions of the Creative Commons Attribution (CC-BY) license (http://creativecommons.org/licenses/by/4.0/).